Well hydraulics theory and data analysis of the constant head test in an unconfined aquifer with the skin effect

Chia-Shyun Chen and Chien-Chieh Chang

Institute of Applied Geology, National Central University, Chung-li, Taiwan

Received 10 June 2002; revised 26 December 2002; accepted 13 February 2003; published 8 May 2003.

[1] In a constant-head test (CHT), groundwater is withdrawn from a well that has a fixed drawdown. Accordingly, the CHT is particularly useful in aquifers of low transmissivity because the constant-head well would not be dewatered owing to overpumping. The problem of interest pertains to a CHT in a homogeneous and anisotropic unconfined aquifer, where water released by the water table decline is assumed to be instantaneous and the skin effect surrounding the constant-head well is represented by a skin factor. A two-dimensional transient well hydraulics model is developed, and its Laplace domain solutions of aquifer drawdown and the constant-head well discharge are determined. It is found that the three distinct segments typically noted in the time drawdown history of a constant-rate test (CRT) are also characteristic of the temporal drawdown variation of the CHT. However, the early time and late time asymptotes conform to the radial flow solution of a CHT in confined aquifers as given by *Hantush* [1964]. Under the late time radial flow conditions the asymptotic solution is in terms of an apparent storage coefficient equal to the sum of the storage coefficient and the specific yield, and a specific mass balance relation exists among the constant-head well discharge, the discharge due to aquifer storage, and the discharge resulted from the water table decline. While aquifer drawdown and the constant-head well discharge are under the influence of well skin, their ratios are free from it. A curve matching method using this ratio is developed to determine the horizontal and the vertical hydraulic conductivities, the storage coefficient, and the specific yield. When the prescribed constant drawdown is not negligibly small in comparison to the initial saturated thickness, aquifer drawdown in late times may be large, and thus a drawdown correction is needed for data analysis. It is found that the Jacob correction for large drawdown of a CRT can also be used for the late drawdown correction in a CHT. *INDEX TERMS:* 1829 Hydrology: Groundwater hydrology; 1894 Hydrology: Instruments and techniques; *KEYWORDS:* constant-head pumping, unconfined aquifers, field data analysis, Laplace domain solutions

Citation: Chen, C.-S., and C.-C. Chang, Well hydraulics theory and data analysis of the constant head test in an unconfined aquifer with the skin effect, *Water Resour. Res.*, *39*(5), 1121, doi:10.1029/2002WR001516, 2003.

1. Introduction

1.1. Unconfined Flow Theories

[2] Pumping in an unconfined aquifer causes the water table to fall, thereby inducing gravity drainage of pore water above the falling water table. This drainage recharges the underlying saturated thickness and influences drawdown evolution. Under constant rate pumping, temporal drawdown variation near the pumping well is characterized by an early time and a late time smooth curves joined by an intermediate time section of slowly varying slope (i.e., the drawdown changing rates are mild). *Boulton* [1955, 1963] postulated that the drainage process associated with the water table decline could be expressed by an exponential decay function of time. This transient function involves an empirical delay index and is incorporated into the mathematical model as an integral source term in the governing equation, which is radially one-dimensional in space. Contrary to Boulton's assumption, *Dagan* [1967] and *Neuman* [1972, 1974] assumed that the drainage of the pore water above the falling water table was instantaneous. *Neuman* [1972, 1974] incorporated this instantaneous drainage into the two-dimensional mathematical model as a vertical recharge term on the boundary condition representative of the water table.

[3] However, detailed field experiments and theoretical analysis indicate that drainage of pore water above the falling water table is transient, and both the radial and vertical flow components occur in saturated thickness [*Nwankwor et al.*, 1992; *Akindunni and Gillham*, 1992; *Narasimhan and Zhu*, 1993; *Moench*, 1994]. In view of this finding, *Moench* [1995] modified Neuman's two-dimensional model by replacing the instantaneous drainage with the Boulton's time decay integral on the water table boundary condition. *Moench* [1997] further expanded this model by adding well bore storage and the skin effect. However, *Narasimhan and Zhu* [1993] pointed out that the transient drainage process associated with the water table decline is mathematically more complicated than the simple exponential relation as proposed by Boulton. *Moench et al.* [2001]

0043-1397/03/2002WR001516

treated this drainage as a finite series of exponential terms, each of which contains one empirical parameter that is to be determined. *Chen and Ayers* [1998], however, employed the *Neuman* [1974] solution and the *Moench* [1995] solution to analyze the same set of CRT data and suggested that the Neuman solution was sufficient for parameter estimation. Therefore how to model this drainage associated with water table decline warrants further research.

1.2. Constant Head Tests

[4] This paper deals with another subject meriting attention; that is, constant head pumping in unconfined aquifers. In a constant head test (CHT), groundwater is withdrawn from a constant-head well at which a fixed water depth (the prescribed constant head) is maintained. Many landfills and contaminated sites are found in shallow unconfined aquifers of low transmissivity, where the conventional constant rate test (CRT) usually is implausible because setting a constant pumping rate to generate significant drawdown without dewatering the pumping well is difficult or even impractical. In this regard, the CHT becomes particularly useful because the constant water depth prevents the well from dewatering due to overpumping. In addition, constant head pumping is typically used to recover light nonaqueous phase liquids [*Abdul*, 1992], or to control off-site migration of contaminated groundwater [*Hiller and Levy*, 1994].

[5] As commonly occurred in a CRT, well bore storage at the pumping well can influence the early time drawdown behavior at the pumping well and at the observation wells. Ignoring well bore storage may lead to the deduction of nonexistent aquifer conditions (e.g., faults, hydrogeological boundaries), or to an analysis of the wrong portion of the transient test data [*Earlougher*, 1977]. *Jargon* [1976] indicated that the negligence of well bore storage can cause an underestimation of transmissivity and an overestimation of storativity, and the larger the well bore storage effect the greater the error will be. The overestimation of storativity can be one to two orders of magnitude [*Mucha and Paulikova*, 1986; *Narasimhan and Zhu*, 1993; *Moench*, 1997]. Therefore if a line sink solution is used to analyze drawdown data of an unconfined aquifer, *Moench* [1994] suggested that storativity not be evaluated using the early time measurements because they may be dominated by well bore storage.

[6] In the CHT well hydraulics theories, well bore storage of the constant-head well is usually neglected in light of a fixed water volume in the well. Under field conditions, however, well bore storage is negligible if the constant head can be rapidly established in a short period of time without generating significant groundwater flow. This is accomplishable when the aquifer has low transmissivity and the well radius is small. If well bore storage cannot be neglected, it may influence the discharge at the constant-head well $Q_w(t)$ and drawdown variations at observation wells h(r, t) in early times. However, the study of such effects is beyond the scope of the current work.

[7] So far, the underlying well hydraulics theories of CHT have been limited to radial flow problems in confined or leaky aquifers. For confined aquifers, *Jacob and Lohman* [1952] gave the solution of $Q_w(t)$, and developed the method of using $h_w/Q_w(t)$ to estimate the storage coefficient S and the transmissivity *T. Hantush* [1964, p. 309] presented the solution of h(r, t) for confined aquifers, while *Hantush* [1964, p. 312] gave the solutions of h(r, t) and $Q_w(t)$ for leaky aquifers. *Mishra and Guyonnet* [1992] developed the method of using $h(r, t)/Q_w(t)$ of the late times of a CHT to estimate T and S. It is important to know that the field data of $Q_w(t)$ is crucial for the parameter estimation. Should $Q_w(t)$ be unavailable, only can the hydraulic diffusivity T/S be determined by using h(r, t) alone [*Hiller and Levy*, 1994; *Uraiet and Raghaven*, 1980]. *Murdoch and Franco* [1994] employed the method of instantaneous source functions to determine the drawdown solutions in a well field involving multiple constant-head wells, where the linear superposition method is applied to the source functions instead of the drawdown functions.

[8] When well skin is taken into account, a number of CHT well hydraulics theories are available for confined aquifers. Assuming that well skin has finite thickness, *Clegg* [1967] employed the *Schapery* [1961] method to determine approximate solutions for different CHT problems. *Uraiet and Raghavan* [1980] found that the infinitesimal thickness skin approach usually used in the CRT is also useful for the CHT problems. Using this approach, *Hurst et al.* [1969] developed the solution for the cumulative discharges of the constant-head well, which is the integration of $Q_w(t)$ with respect to time. *Chen and Chang* [2002] performed a constant head injection test, in which surface water was injected into the well in an excessive amount such that the well was overflowed to maintain the constant head. The difference between the injection rates and the overflow rates gives the cumulative discharges, which were used to estimate T and S. A partially penetrating constant-head well can be simulated as a mixed type boundary condition, in which the Dirichlet or the Cauchy condition is stipulated along the well screen while the Neumann condition of no flux for the unscreened part. For the mixed type boundary problems, *Cassiani et al.* [1999] used the dual integral equation method to find solutions for a confined aquifer of infinite thickness, and *Chang and Chen* [2002, 2003] developed an integral transform approach to determine the solutions for a confined aquifer of finite thickness.

1.3. Purposes

[9] As discussed above, all the well hydraulics theories for constant head pumping are not for unconfined aquifers. Therefore it is the purposes of this paper to develop a well hydraulic theory for constant head pumping in unconfined aquifers and to establish a parameter estimation method.

2. Theoretical Analysis

2.1. Model and Solutions

[10] The problem of interest pertains to the withdrawal of groundwater from a well maintained at a constant drawdown h_w in a homogeneous and anisotropic unconfined aquifer of infinite areal extent. Sealed at the bottom, the constant-head well fully penetrates the saturated thickness and has no well bore storage. Although well bore storage is neglected, the constant-head well must be assumed as a cylindrical sink wherein the radius has a direct influence on $Q_w(t)$. Here an effective well radius r_w, as measured from the well center to the outer edge of the filter pack, is assumed for the constant-head well. The possible well skin surrounding the gravel pack is assumed to have infinitesimal thickness, and its effect is taken into account by using a constant skin factor S_k. As for the observation wells, the radius is assumed to be infinitesimal while well bore storage is neglected.

[11] It is further assumed that aquifer drawdown is everywhere small in comparison to the initial saturated thickness b such that b can be considered as constant. Groundwater withdrawn is assumed to derive from aquifer storage of a constant storativity S_s, and drainage from the water table decline. In the absence of a well-established transient relation for this drainage process, the Neuman's instantaneous modeling approach is adopted. As a result, the transient two-dimensional flow model is formulated as follows, and all symbols are defined in Notation unless otherwise noted.

$$K_r\left[\frac{\partial^2 h}{\partial r^2}+\frac{1}{r}\frac{\partial h}{\partial r}\right]+K_z\frac{\partial^2 h}{\partial z^2}=S_s\frac{\partial h}{\partial t}\qquad r_w\le r\le\infty,\quad 0\le z\le b \tag{1}$$

$$h(r,z,0)=0 \tag{2}$$

$$h(r_w,t)-r_wS_k\left.\frac{\partial h}{\partial r}\right|_{r=r_w}=h_w \tag{3}$$

$$h(\infty,z,t)=0 \tag{4}$$

$$\left.\frac{\partial h}{\partial z}\right|_{z=0}=0 \tag{5}$$

$$K_z\left.\frac{\partial h}{\partial z}\right|_{z=b}=-S_y\left.\frac{\partial h}{\partial t}\right|_{z=b} \tag{6}$$

where the vertical distance is positive upward with z = 0 at the bottom of the aquifer, and the water table locates at z = b. In an appropriate dimensionless form, the above model is solved by the Laplace transform and the separation of variables technique, as discussed in Appendix A. For h(r, z, t), the associated dimensionless solution in the Laplace domain is

$$h_D(\rho,\zeta,\tau)=L^{-1}\left\{\frac{2}{p}\sum_{n=1}^{\infty}\frac{K_0(\chi_n\rho)}{K_0(\chi_n)+S_k\chi_nK_1(\chi_n)}\frac{\cos(\varepsilon_n\zeta)}{\lambda_n\cos\varepsilon_n}\right\} \tag{7}$$

where $\lambda_n = 1 + \sigma p/\beta + (\varepsilon_n^2\beta/\sigma p)$, $\sigma = S_y/S$, $\beta = (K_z/K_r)(r_w^2/b^2)$, ε_n is the nth positive root of (A18), and p is the Laplace transform parameter for the dimensionless time τ. The symbol $L^{-1}\{\}$ represents the Laplace inversion operator, and the numerical method given by *Stehfest* [1970] is employed to calculate the Laplace inversions presented in this paper.

[12] Depth specific drawdown h(r, z, t) is particularly useful in the investigation of vertical flow components, and its measurement is typically made use of piezometers located at various depths and distances from the constant-head well. Under field conditions, however, fully penetrating observation wells are frequently employed to yield average drawdown over the screen length. The average drawdown for $h_D(\rho, \zeta, \tau)$ is

$$h_D^*(\rho,\tau)=\int_0^1 h_D(\rho,\zeta,\tau)d\zeta = L^{-1}\left\{\frac{2\sigma}{\beta}\sum_{n=1}^{\infty}\frac{K_0(\chi_n\rho)}{K_0(\chi_n)+S_k\chi_nK_1(\chi_n)}\frac{1}{\lambda_n\varepsilon_n^2}\right\} \tag{8}$$

[13] As manifested by the boundary condition of (3), there is a discontinuity in drawdown across r_w (i.e., $\rho = 1$) due to well skin. As such, the evaluation of (8) at $\rho = 1$ gives aquifer drawdown at $\rho = 1^+$, which represents the "outer" well skin surface in contact with aquifer materials. On the other hand, $\rho = 1^-$ denotes the "inner" well skin surface exposing to the constant-head well, on which the prescribed constant head is imposed. The drawdown difference between $\rho = 1^+$ and $\rho = 1^-$ is the local head drop caused by well skin. Despite the discontinuity in drawdown, the flow rate across $\rho = 1$ is continuous because of the infinitesimal thickness assumed for well skin. Thus the constant-head well discharge can be determined by applying Darcy's law to (8) for $\rho = 1$; that is,

$$Q_w(\tau)=-\int_0^1\left.\frac{\partial h_D}{\partial\rho}\right|_{\rho=1}d\zeta = L^{-1}\left\{\frac{2\sigma}{\beta}\sum_{n=1}^{\infty}\frac{\chi_nK_1(\chi_n)}{K_0(\chi_n)+S_K\chi_nK_1(\chi_n)}\frac{1}{\lambda_n\varepsilon_n^2}\right\} \tag{9}$$

2.2. Influence of Aquifer Storage and Water Table Decline

[14] The flux from aquifer storage over the entire saturated thickness at a specific distance is

$$q_s(\rho,\tau)=\frac{\partial h_D^*}{\partial\tau}=L^{-1}\left\{\frac{2\sigma p}{\beta}\sum_{n=1}^{\infty}\frac{K_0(\chi_n\rho)}{K_0(\chi_n)+S_k\chi_nK_1(\chi_n)}\frac{1}{\varepsilon_n^2\lambda_n}\right\} \tag{10}$$

[15] At the water table (i.e., $\zeta = 1$), the vertical drainage flux due to the water table decline at a specific distance is

$$q_{Sy}(\rho,\tau)=\sigma\left.\frac{\partial h_D}{\partial\tau}\right|_{\zeta=1}=L^{-1}\left\{2\sigma\sum_{n=1}^{\infty}\frac{K_0(\chi_n\rho)}{K_0(\chi_n)+S_k\chi_nK_1(\chi_n)}\frac{1}{\lambda_n}\right\} \tag{11}$$

Figure 1 shows the distribution curves of $q_{sy}(\rho, \tau)$ and $\sigma q_s(\rho, \tau)$ for the near field (e.g., $\rho = 10$) and the far field (e.g., $\rho = 1000$), where the skin effect is neglected. It is seen that either aquifer storage or the water table decline produces only a finite amount of water that decreases with increasing distance. At each distance, the curve of $q_{sy}(\rho, \tau)$ lags behind that of $\sigma q_s(\rho, \tau)$, indicating a delayed water table response. As τ increases to about 10^6, the curves of $q_{sy}(\rho, \tau)$ and $\sigma q_s(\rho, \tau)$ merge in one; that is, $q_{sy}(\rho, \tau)$ equals $\sigma q_s(\rho, \tau)$. In reference to (10) and (11), the equality of $q_{sy}(\rho, \tau)$ and $\sigma q_s(\rho, \tau)$ signifies that $\partial h_D^*/\partial\tau$ is equal to $\partial h_D/\partial\tau$ evaluated at $\zeta = 1$, resulting in negligible vertical flow components in saturated thickness. Thus the groundwater flow field becomes radial in late times, provided that the test duration is sufficiently long. The onset time of this radial flow is independent of the distance, but is dependent on σ and β; e.g., for the current case where $\sigma = 10$ and $\beta = 10^{-4}$, it is about $\tau = 10^6$.

[16] Since the total groundwater flux $q(\rho, \tau)$ equals the sum of $q_s(\rho, \tau)$ and $q_{sy}(\rho, \tau)$, under the late time radial flow condition $q(\rho, \tau)$ becomes $(1 + \sigma)q_s(\rho, \tau)$, which has a dimensional form of $(S + S_y)\partial h(r, t)/\partial t$. This dimensional expression is equivalent to the groundwater flux derived

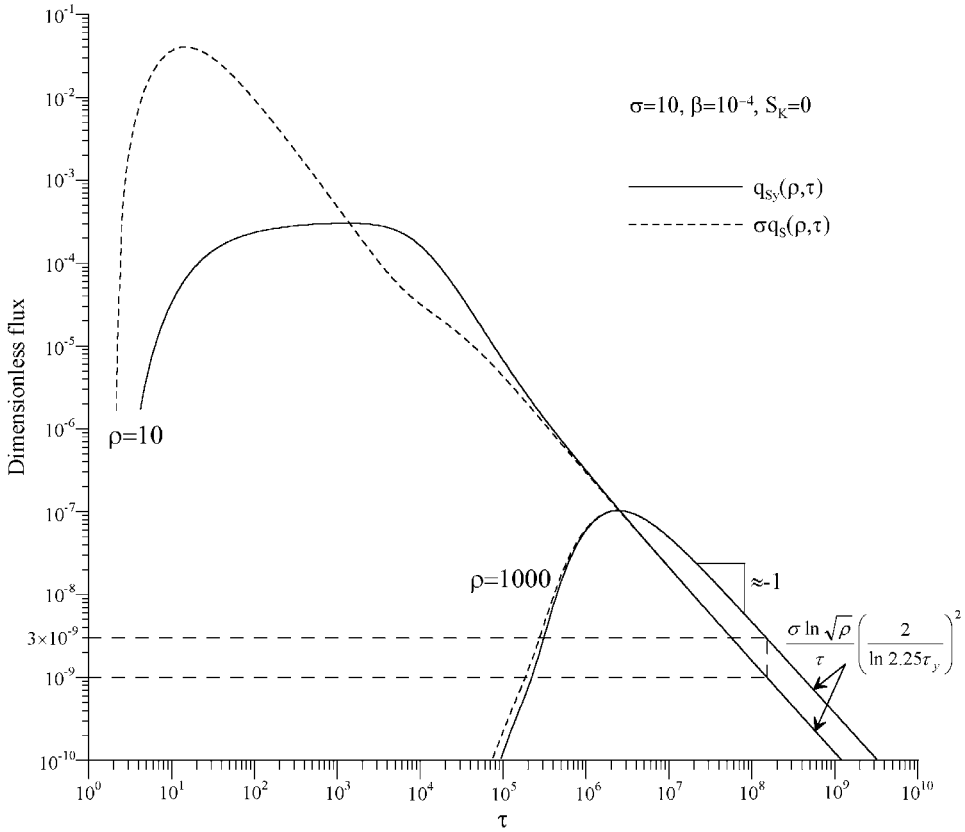

Figure 1. Distribution curves of $q_{sy}(\rho, \tau)$ and $\sigma q_s(\rho, \tau)$ at $\rho = 10$ and $\rho = 1000$.

from aquifer storage that has a storage coefficient in a magnitude equal to the sum of S and S_y. Despite the different physical meanings of these two parameters, $S + S_y$ can be considered as an apparent storage coefficient, S_a, for the late time radial flow. This additive property of S and S_y is also observed in the late time groundwater flow of *Neuman* [1972] model as discussed by *Gambolati* [1976]. As a result, a new dimensionless time τ_y can be defined in terms of S_a; that is, $\tau_y = Tt/(r_w^2 S_a)$ or $\tau/(1 + \sigma)$.

[17] After the establishment of the late time radial flow field, $q_{sy}(\rho, \tau)$ can be approximated by the following formula

$$q_{sy}(\rho, \tau) = \frac{\sigma \ln \sqrt{\rho}}{\tau} \left(\frac{2}{\ln 2.25\tau_y} \right)^2 \tag{12}$$

which is obtained by applying the late time approximate drawdown solution, as shown below in (22), to (11). The square term in (12) changes slowly for a large τ_y, and thus the logarithmic variation of $q_{sy}(\rho, \tau)$ versus τ approaches a straight line of a slope close to -1, as illustrated in Figure 1. Furthermore, the vertical separation of the two straight lines of $q_{sy}(\rho, \tau)$ is 3, resulting in $q_{sy}(1000, \tau)$ being three times as large as $q_{sy}(10, \tau)$. By (12), the ratio of $q_{sy}(\rho_1, \tau)$ to $q_{sy}(\rho_2, \tau)$ is $\ln\rho_1/\ln\rho_2$, provided that σ is constant. Due to $q_{sy}(\rho, \tau) = \sigma q_s(\rho, \tau)$ and $q(\rho, \tau) = (1 + \sigma) q_s(\rho, \tau)$, this ratio also applies to $q(\rho, \tau)$ and $q_s(\rho, \tau)$; that is,

$$\frac{q(\rho_1, \tau)}{q(\rho_2, \tau)} = \frac{q_{sy}(\rho_1, \tau)}{q_{sy}(\rho_2, \tau)} = \frac{q_s(\rho_1, \tau)}{q_s(\rho_2, \tau)} = \frac{\ln \rho_1}{\ln \rho_2} \tag{13}$$

[18] In reference to (6) or its dimensionless form (A6), a larger S_y (hence a larger σ) connotes that more water is available for a longer drainage process, and a larger K_z (hence a larger β) results in a greater vertical drainage flux. As illustrated in Figure 2a, at $\rho = 10$, the area under the curve of $\beta = 10^{-3}$ is larger than that of the other two curves of $\beta = 10^{-4}$, indicating that more water is released for $\beta = 10^{-3}$. Thus a larger K_z is more conducive to discharge from the water table decline. On the other hand, when β is maintained at 10^{-4}, the two curves of different σ are coincident for a period of time, during which the influence of σ is negligible. Then, the influence of σ takes effect and causes the merged curve to ramify. The branch of $\sigma = 10$ decreases faster than that of $\sigma = 100$ because of less water available for drainage from the water table decline.

[19] In the far field, the aquifer materials begin to respond to water withdrawal after such a long period of time that the late time radial flow has already been established. This can be observed in Figure 2b, where the two curves of $\beta = 10^{-3}$ and 10^{-4}, at $\rho = 2000$, coincide for the complete response time. Also noted in Figure 2b is that the curves of $\sigma = 10$ and $\sigma = 100$ are presented in the same response time span due to the use of τ_y, which assimilates the temporal influence of σ through its definition of $\tau/(1 + \sigma)$.

2.3. Mass Balance Analysis

[20] During a CHT, the hydraulic gradient across the well screen surface is the largest at the onset of groundwater withdrawal and then decreases as the cone of depression expands, and thus the constant-head well discharges $Q_w(t)$

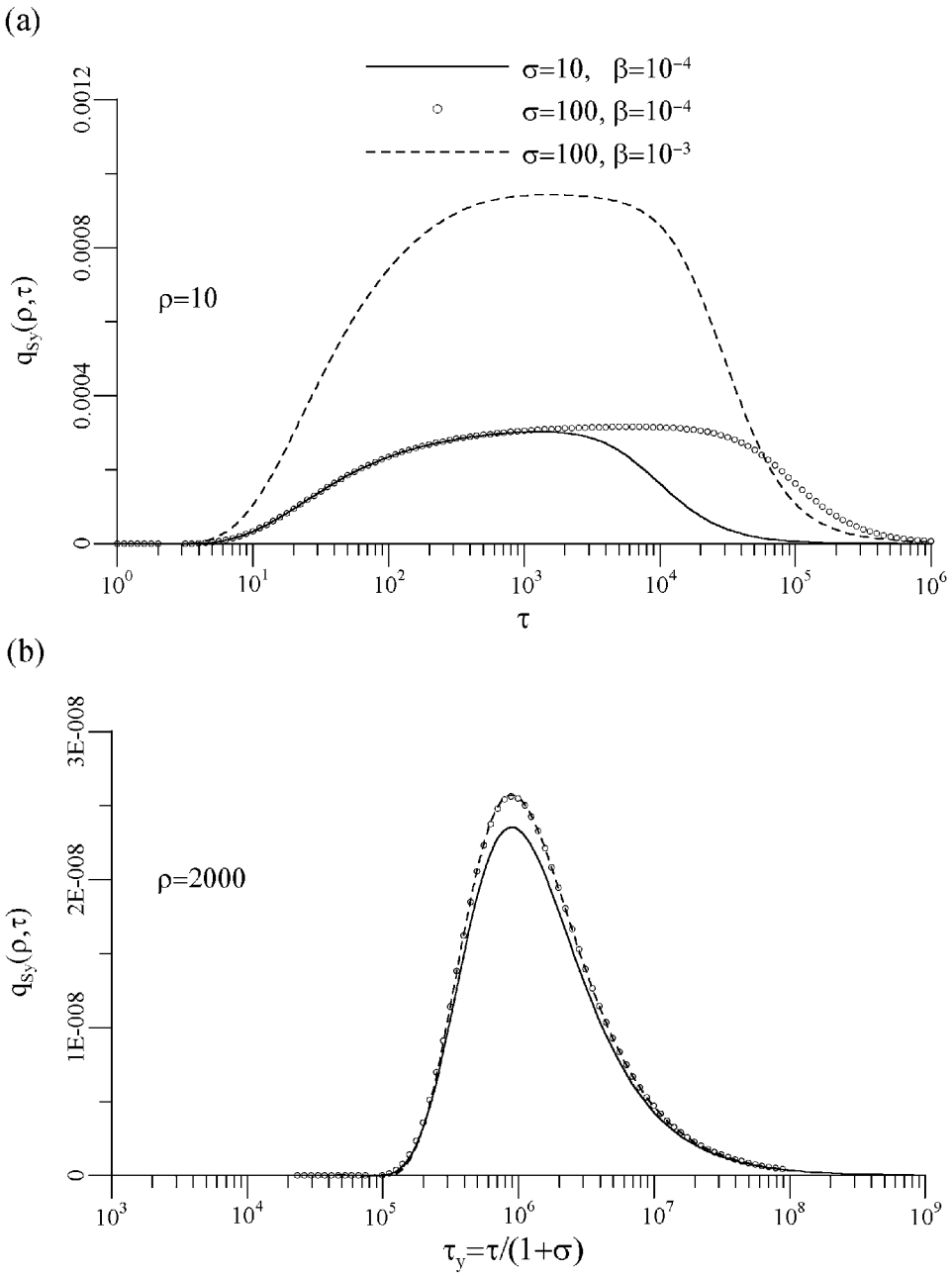

Figure 2. Influence of σ and β on $q_{sy}(\rho, \tau)$ at (a) ρ = 10 and (b) ρ = 2000.

decrease with time. Although the cone of depression expands with time, its extent can be effectively assumed to change from ρ = 1 to infinity in calculating the following mass balance relation

$$Q_w(\tau) = Q_s(\tau) + Q_{sy}(\tau) \tag{14}$$

where

$$Q_S(\tau) = \int_1^\infty q_S(\rho,\tau)\rho d\rho = L^{-1}\left\{2\sum_{n=1}^{\infty}\frac{K_1(\chi_n)}{K_0(\chi_n)+S_k\chi_n K_1(\chi_n)}\frac{\sigma}{\chi_n\lambda_n}\frac{p}{\beta\varepsilon_n^2}\right\} \tag{15}$$

$$Q_{Sy}(\tau) = \int_1^\infty q_{Sy}(\rho,\tau)\rho d\rho = L^{-1}\left\{2\sum_{n=1}^{\infty}\frac{K_1(\chi_n)}{K_0(\chi_n)+S_k\chi_n K_1(\chi_n)}\frac{\sigma}{\chi_n\lambda_n}\right\} \tag{16}$$

[21] The mass balance relation of (14) is graphically displayed in Figure 3, where the curve of $Q_w(\tau)$ is composite of the curves of $Q_s(\tau)$ and $Q_{sy}(\tau)$. Three distinct stages of $Q_w(\tau)$ are manifested in early times ($\tau < 1$), intermediate times ($1 < \tau < 10^6$), and late times ($\tau > 10^6$). In early times, $Q_{sy}(\tau)$ is negligibly small and $Q_s(\tau)$ essentially supplies the whole $Q_w(\tau)$. In the intermediate times, both $Q_s(\tau)$ and $Q_{sy}(\tau)$ contribute to $Q_w(\tau)$. While $Q_s(\tau)$ continuously

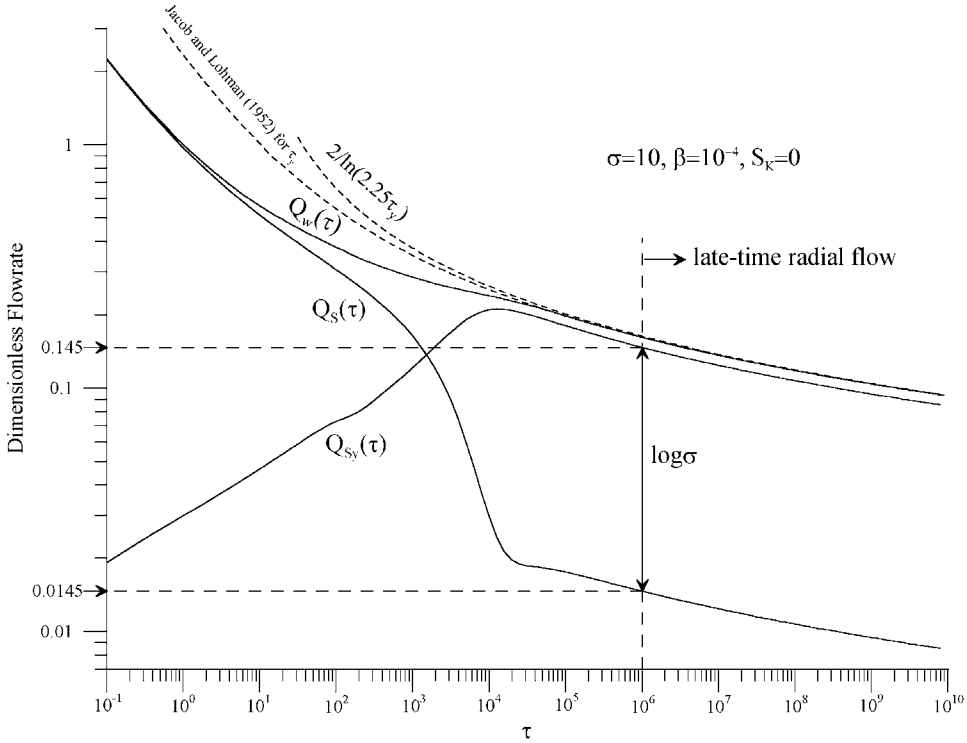

Figure 3. Graphical representation of the mass balance relation of $Q_w(\tau)$ being the sum of $Q_{Sy}(\tau)$ and $Q_S(\tau)$.

decreases, $Q_{sy}(\tau)$ is in increase. But, $Q_{sy}(\tau)$ cannot increase without bound because $Q_w(\tau)$ is finite. Accordingly, the increasing $Q_{sy}(\tau)$ turns to decrease when τ is about 2×10^4, at which the decreasing rate of $Q_s(\tau)$ correspondingly slows down. Then, as τ is greater than about 10^6, the late time radial flow condition prevails and the three curves of $Q_w(\tau)$, $Q_s(\tau)$ and $Q_{sy}(\tau)$ are parallel. In noting that σ is 10, the two parallel curves of $Q_{sy}(\tau)$ and $Q_s(\tau)$ are separated by one log cycle; that is, $Q_{sy}(\tau)$ is σ times as large as $Q_s(\tau)$, substantiating the relation of $q_{sy}(\rho, \tau) = \sigma q_s(\rho, \tau)$ discussed above. As a result, the mass balance relation (14) of the late time radial flow becomes

$$Q_w(\tau) = (1+\sigma)Q_s(\tau) = \left(\frac{1+\sigma}{\sigma}\right)Q_{sy}(\tau) \tag{17a}$$

or

$$Q_w(t) = \frac{S_a}{S}Q_s(t) = \frac{S_a}{S_y}Q_{sy}(t) \tag{17b}$$

[22] As τ further increases to be greater than about 5×10^6, $Q_w(\tau)$ can be simplified to

$$Q_w(\tau) = 2/\left(\ln 2.25\tau_y + 2S_k\right) \tag{18}$$

which was originally given by *Clegg* [1967, equation B-13]. In accordance with (18), if S_k is zero, the square term in (12) can be expressed as $Q_w(\tau)^2$.

2.4. Drawdown Distribution

[23] The transient variations of depth specific drawdown determined by (7) are illustrated in Figure 4, where S_k is assumed to be zero. The vertical flow components at the three distances disappear after τ is greater than 10^6, indicating that the late time radial flow field is established for τ larger than 10^6. For τ less than 10^6, however, the vertical flow components at a shorter distance (e.g., ρ = 10 or 100) are unimportant in early times but significant in intermediate times. For example, at ρ = 10, there are no vertical flow components for τ less than about 20. As discussed in Appendix B, drawdown for small τ can be approximated by

$$h_e(\rho,\tau) = L^{-1}\left\{\frac{1}{p}\frac{K_0\left(\rho\sqrt{p}\right)}{K_0\left(\sqrt{p}\right) + S_K\sqrt{p}K_1\left(\sqrt{p}\right)}\right\} = L^{-1}\{H_e(\rho,p)\} \quad \text{for } 0 \le \zeta < 1 \tag{19}$$

and

$$h_e(\rho,\tau) = 0, \qquad \text{for } \zeta = 1 \tag{20}$$

The condition set forth by (20) indicates that the head on the water table remains unchanged, and thereby no water is released from the zone above the water table. The condition of (19), however, shows a radial flow in saturated thickness below the water table. At early times, therefore, water withdrawn essentially comes from aquifer storage near the constant-head well, where a radial groundwater flow takes place. When S_k = 0, early time drawdown conforms to the *Hantush* [1964, p. 309] solution as displayed in Figure 4.

[24] When τ is greater than 20, water released by the water table decline induces downward vertical flow components in saturated thickness, causing the early time asymptote to branch off. Among the various depths, the vertical flow takes the longest time to reach the bottom of the aquifer, and thus the drawdown curve of ζ = 0 departs

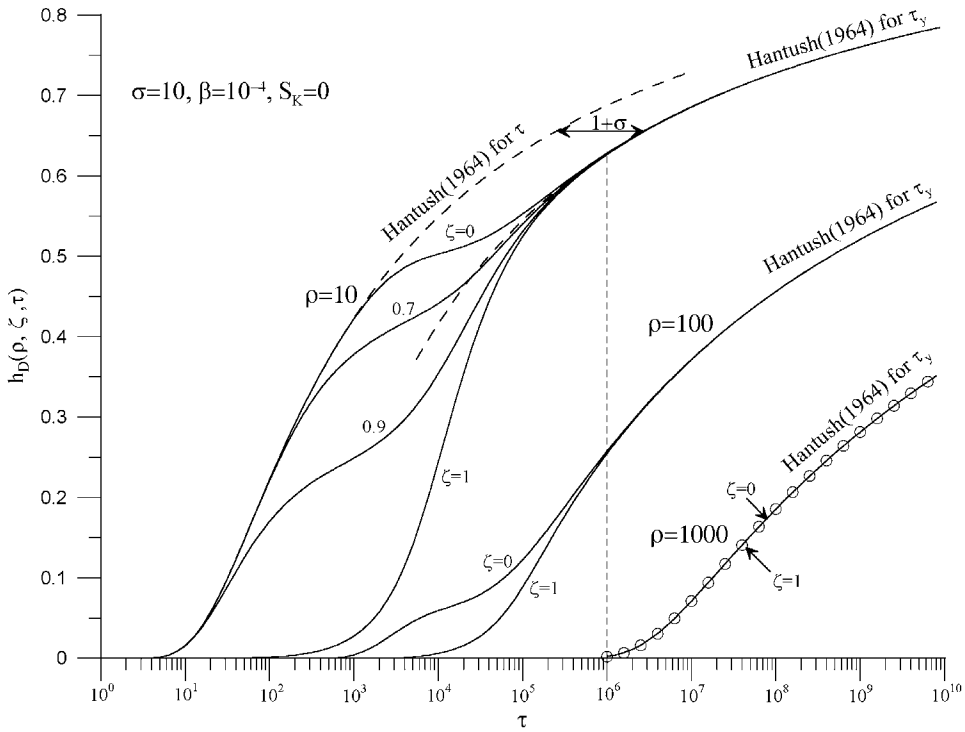

Figure 4. Depth-specific drawdown variations at ρ = 10, 100 and 1000.

from the early time asymptote the latest. At the water table, however, the response lags behind the drawdown at the rest of the aquifer due to the delayed water table response discussed above.

[25] The drawdown curves of different depths diverge for a period of time during which $q_{sy}(\rho, \tau)$ is in increase. Then, they begin to converge as $q_{sy}(\rho, \tau)$ starts to decrease. When τ is greater than 10^6, the vertical flow components become negligibly small, and the drawdown curves of different depths merge in a single one representative of the late time radial flow. As discussed in Appendix B, the late time drawdown can be approximated by

$$h_l(\rho,\tau) = L^{-1}\left\{\frac{1+\sigma}{P}\frac{K_0\left(\rho\sqrt{P}\right)}{K_0\left(\sqrt{P}\right)+S_K\sqrt{P}K_1\left(\sqrt{P}\right)}\right\} \quad \text{for } 0 \le \zeta \le 1$$
$$= (1+\sigma)L^{-1}\{H_e(\rho,p)\} \tag{21}$$

in which $P = (1 + \sigma)p$, and $H_e(\rho, P)$ represents the Laplace domain solution of (19) in terms of $(1 + \sigma)p$. The equality of the last two terms of (21) reveals that the Laplace transform solution of late times is related to the Laplace transform solution of early times through the shifting rule of the Laplace transform [e.g., *Churchill*, 1972, p. 458]. As a result, the late time approximate solution is the early time approximate solution in terms of τ_y; that is, $h_l(\rho, \tau) = h_e(\rho, \tau_y)$. Therefore the early time asymptote and the late time asymptote are parallel curves with a horizontal separation equal to $(1 + \sigma)$, as shown in Figure 4. As τ continues to increase, $h_l(\rho, \tau)$ can be further simplified by applying the *Schapery* [1961] method to (21), and the result is

$$h_l(\rho,\tau) = \frac{\ln 2.25\tau_y/\rho^2}{\ln 2.25\tau_y + 2S_k} \tag{22}$$

which is valid for τ/ρ^2 greater than about 1,000 for the current case. However, it should be noted that (22) is applicable after a certain time limit that varies with σ and β and increases with the distance.

2.5. Skin Effect

[26] For a CHT, $h^*(r, t)$ and $Q_w(t)$ are continuously under the influence of well skin during the entire test period. However, when the ratio $h^*(r, t)/Q_w(t)$ is taken into account, the skin effect can be ignored without causing significant error. As shown in Figure 5, the influence of the skin effect on $h^*_D(\rho, \tau)/Q_w(\tau)$ is quantified. For $\rho > 1$ the difference between the curves of $S_k = 0$ and 100 is less than about 1%. When τ/ρ^2 is greater than about 1000, these curves merge in one that can be represented as the ratio of (22) to (18), namely,

$$h^*_D(\rho,\tau)/Q_w(\tau) = 0.5\ln\left(2.25\tau_y/\rho^2\right) \tag{23}$$

in which the skin factor disappears. The dimensional form of (23) is as follows:

$$\frac{h^*(r,t)}{Q_w(t)} = \frac{0.183}{T}\log\left(\frac{2.25Tt}{r^2S_a}\right) \tag{24}$$

According to (24), in late times there is a linear relation between $h^*(r, t)/Q_w(t)$ and logarithmic time. Thus the slope and the intercept of this straight line can be used to determine T and S_a by the well-known semilog method developed by *Cooper and Jacob* [1946]. If S_a is changed to S, (24) reduces to the late time approximate solution given by *Hantush* [1964] or *Mishra and Guyonnet* [1992] for confined conditions.

[27] On the other hand, however, $h_w/Q_w(t)$ or $1/Q_w(\tau)$, is not free from the skin effect at any time because the

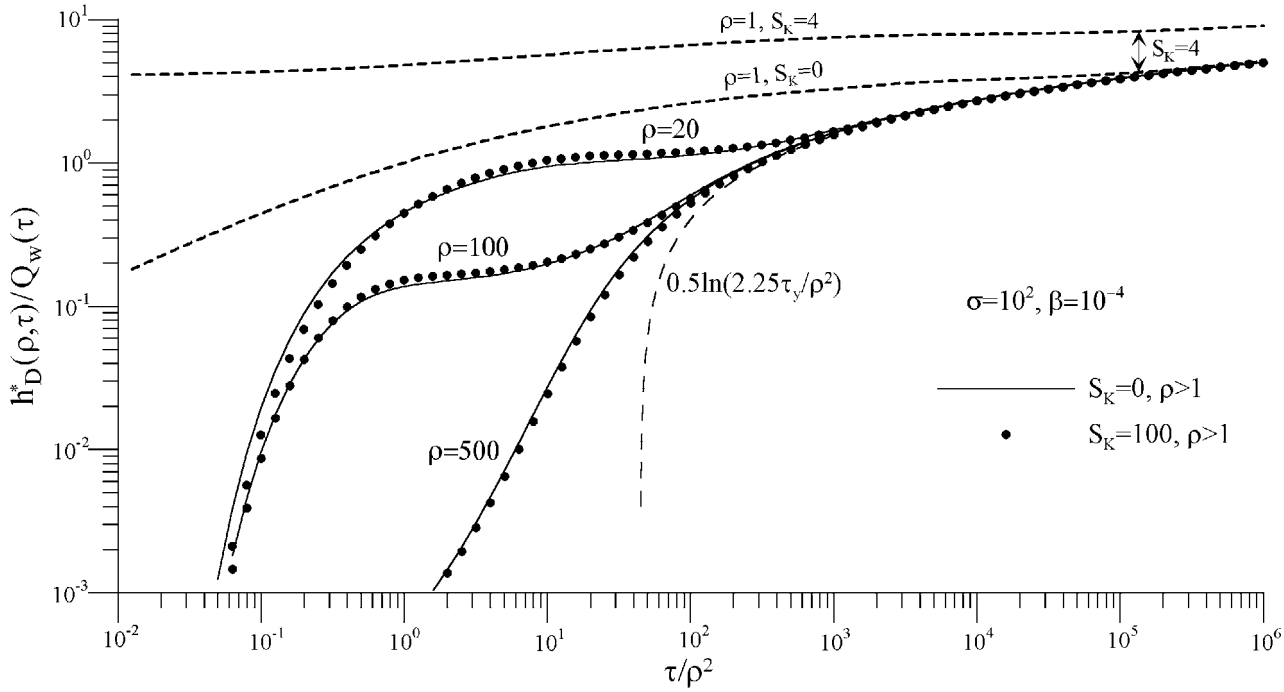

Figure 5. Influence of the skin effect on the ratios of aquifer drawdown to the flow rate at the constant-head well ($\rho > 1$) and on the ratios of the constant head to the flow rate at the constant-head well ($\rho = 1$).

constant-head well discharge is continuously under the influence of well skin. As verified in Figure 5, the two curves of $1/Q_w(\tau)$ marked by $\rho = 1$ and $S_k = 0$ and 4, respectively, are distinctly different at any times. In late times, however, they become parallel with a vertical separation equal to S_k. By taking the inverse of (18), these parallel curves can be expressed by

$$1/Q_w(\tau) = 0.5\ln(2.25\tau_y) + S_k \tag{25a}$$

or

$$\frac{h_w}{Q_w(t)} = \frac{0.183}{T}\log\left(\frac{2.25Tt}{r_w^2 S_a}\right) + \frac{S_k}{2\pi T} \tag{25b}$$

The only difference between (24) and (25b) is the last term $S_k/(2\pi T)$ in (25b). This extra term does not change the slope of the late time straight line but affects its intercept. Since S_k is unknown a priori, the late time data of $h_w/Q_w(t)$ can be used to estimate T but not S_a if well skin exists. In general, it is suggested to use specific drawdown of the observation well for parameter estimation, especially when well skin is known to exist around the constant-head well.

[28] Whether well bore storage and well skin are considered or not, the late time drawdown solution of a CRT in unconfined aquifers conform to the Theis solution in terms of τ_y [*Moench*, 1997; *Narasimhan and Zhu*, 1993; *Gambolati*, 1976]. When the pumping time is sufficiently long, this solution can be approximated by

$$\frac{h(r,t)}{Q} = \frac{0.183}{T}\log\left(\frac{2.25Tt}{r^2 S_a}\right) \tag{26}$$

of which the right hand side is identical to that of (24). Therefore for sufficiently long times, the ratios of h(r, t)/Q from a CRT and the ratios of $h(r, t)/Q_w(t)$ from a CHT should be the same, provided that the same wells are used in the two tests. This result is also noted for the confined condition, as reported by *Jacob and Lohman* [1952].

2.6. Correction for Large Drawdown

[29] If h_w is large in comparison to b, the water table in the neighborhood of the constant-head well may decline significantly in late times. In this case, the assumption of constant aquifer thickness being equal to b is violated. Thus it is required that the late drawdown data are corrected prior to the data analysis. For a CRT, *Jacob* [1944] suggested that before the data analysis the drawdown data be corrected according to

$$h' = h_l - \left(h_l^2/2b\right) \tag{27}$$

where $h_l(r, t)$ is the late time aquifer drawdown. Furthermore, *Neuman* [1975] noted that the Jacob correction is strictly applicable only to the late drawdown data associated with the radial flow conditions, and is not applicable to the early and intermediate data.

[30] Under the Dupuit assumptions, the governing equation for the late time radial flow of variable aquifer thickness is nonlinear as shown below

$$\frac{1}{r}\frac{\partial}{\partial r}\left[r(b-h_l)\frac{\partial h_l}{\partial r}\right] = \frac{S_a}{K_r}\frac{\partial h_l}{\partial t} \tag{28}$$

Substitution of (27) into (28) yields

$$\frac{\partial^2 h'}{\partial r^2} + \frac{1}{r}\frac{\partial h'}{\partial r} = \frac{S_a'}{T}\frac{\partial h'}{\partial t} \tag{29}$$

where

$$S_a' = \frac{S_a b}{b - h_l} \tag{30}$$

[31] In spite of the dependence on $h_l(r, t)$, S_a' is treated as a constant in the determination of the analytical solution of (29). For the current study, the initial and boundary conditions appropriate for (29) are (2), (3), and (4) in terms of h'. The expressions of (2) and (4) in terms of h' remain as their original forms. In the absence of the skin effect, however, (3) is changed to

$$h'(r_w, t) = H_w = h_w - \left(h_w^2/2b\right) \tag{31}$$

Because the skin effect on $h_l(r, t)/Q_w(t)$ is minimal, the impact of neglecting the skin effect on $h'(r, t)/Q_w(t)$ is negligible. Furthermore, the measured $Q_w(t)$ requires no correction because under the radial flow condition $Q_w(t)$ in terms of h_l or h' is the same, as demonstrated by *Neuman* [1975]. As a result, the solution of (29) subject to (2) and (4) in terms of h' and (31) is the *Hantush* [1964] solution, which is the late time asymptote of (7) or (8). Therefore the Jacob correction is also applicable to correcting the late time CHT drawdown data.

3. Parameter Estimation

3.1. Methodology

[32] A curve matching method using the observation well specific drawdown is developed to estimate the four parameters; namely, S (or S_s), S_y, K_r, and K_z. The development is primarily based on three facts substantiated in the above analysis; that is, (1) the possible skin effect can be neglected in specific drawdown of the observation well without causing significant error, (2) the early time groundwater flow is purely radial with water derived from aquifer storage while the late time flow is late time radial of an apparent storage coefficient S_a, and (3) the vertical flow components are most pronounced in intermediate times. Accordingly, S, S_y, and K_r are determined by the early and the late time data, while K_z is estimated by the intermediate-time data.

[33] Two kinds of type curves, types A and B, are required in the curve matching method. Both of them are logarithmic representation of $h_D^*(\rho, \tau)/Q_w(\tau)$ versus τ_y for the dimensionless radial distance between the constant-head well and the observation well of interest. To determine S, S_y, and K_r, type A curves are prepared by using various σ and an arbitrary β. The arbitrariness of β is not problematic because it has little influence on drawdown in early and late times. In the construction of type A curves β can be taken as $(r_w/b)^2$ by assuming $K_r = K_z$ in its definition of $(K_z/K_r)(r_w/b)^2$. With the use of τ_y, type curves of different σ are grouped into one curve in late times such that a unique S_a can be appropriately determined. In early times, however, type A curves are distinguished by σ, and thus the σ associated with the field data can be properly identified. The curve matching process using type A curves generates sufficient information for a unique determination of S, S_y, and K_r. Then, type B curves are prepared for various β and the known σ. They are used to match the field data with an emphasis on intermediate times to find β. Once β is found, K_z can be determined.

[34] *Jones et al.* [1992] performed a 24-hour CHT in shallow weathered glacial till of low clay content and high sand content. A total of 15 observation wells were used, but only four of them are taken into account in the current study. These four observation wells are located at 0.87m, 1.8 m, 2.71m and 3.62 m in a radial line from the constant-head well, which had been maintained at constant drawdown of 1.5 m during the test. Each borehole of the wells was drilled 4.6 m deep from the ground surface with a 102 mm diameter solid stem auger. Schedule 40 PVC of 5.1 cm diameter was used for the well screen and casing, and the bottom 3.05 m of the borehole was screened with 0.25 mm slotted screen. Pea gravel was used to fill the annulus of the bottom 3.4 m of the borehole. Taking the gravel pack as the effective screen length, the constant-head well has an effective well radius of 5.1 cm, and all the wells fully penetrate the weathered till whose saturated thickness was 2.5m. Details of the field conditions and the site hydrogeology are given by *Jones et al.* [1992]. Here field data of $Q_w(t)$ and $h^*(r, t)$ of the four observation wells given in Figures 3 and 6 of *Jones et al.* [1992] are digitized for the current data analysis using the MapInfo system.

[35] Because h_w is 60% of b, the late drawdown data require the Jacob correction. The onset time of the late time radial flow is dependent on σ and β that are unknown before the parameter estimation work; Therefore it is determined by matching the dimensionless type curve of the *Hantush* [1964] solution with drawdown measured at large times. For the four observation wells, it is found that drawdown measured after 260 minutes fall on the Hantush type curve. Thus the Jacob correction is made to those data points. The difference between the corrected and measured drawdowns decreases with the increasing distance; e.g., at r = 0.87 m the measured drawdown at the end of the CHT is 38.58 cm while the corrected one is 35.60 cm, and at r = 3.62 m the maximum measured drawdown is 14.06 cm while the corrected one is 13.67 cm.

[36] In the determination of S_a from S_a', the variable $h_l(r, t)$ in (30) needs to be replaced by a constant "representative drawdown". For example, *Jones et al.* [1992] stated "it is recommended [*Bear*, 1979] that the specific yield (i.e., S_a herein) be computed by using the drawdown at the end of the pumping test at the geometric mean radius of the observation wells." Since such a drawdown is unavailable at the CHT site, it is proposed herein to use the average of the mean square roots of the drawdown data at the four observation wells. The mean square roots of the four sets of drawdown data are respectively, 25.1 cm, 15.6 cm, 11.0 cm, and 6.7 cm. The average of them is 14.6 cm, resulting in $S_a = 0.942 S_a'$.

[37] In the following discussion, the procedure of the curve matching method is explained using the field data at r = 0.87 m (i.e., ρ = 17.1). The procedure consists the following steps.

[38] 1. Plot the field data of $h^*(r, t)/Q_w(t)$ against time on logarithmic paper. Now the corrected drawdown is used for t greater than 260 minutes. Prepare type A curves on logarithmic paper of the same scale as used for the field data curve. Here type A curves are prepared for ρ = 17.1 and various σ. The value for β determined from $(r_w/b)^2$ is 4.16×10^{-4}.

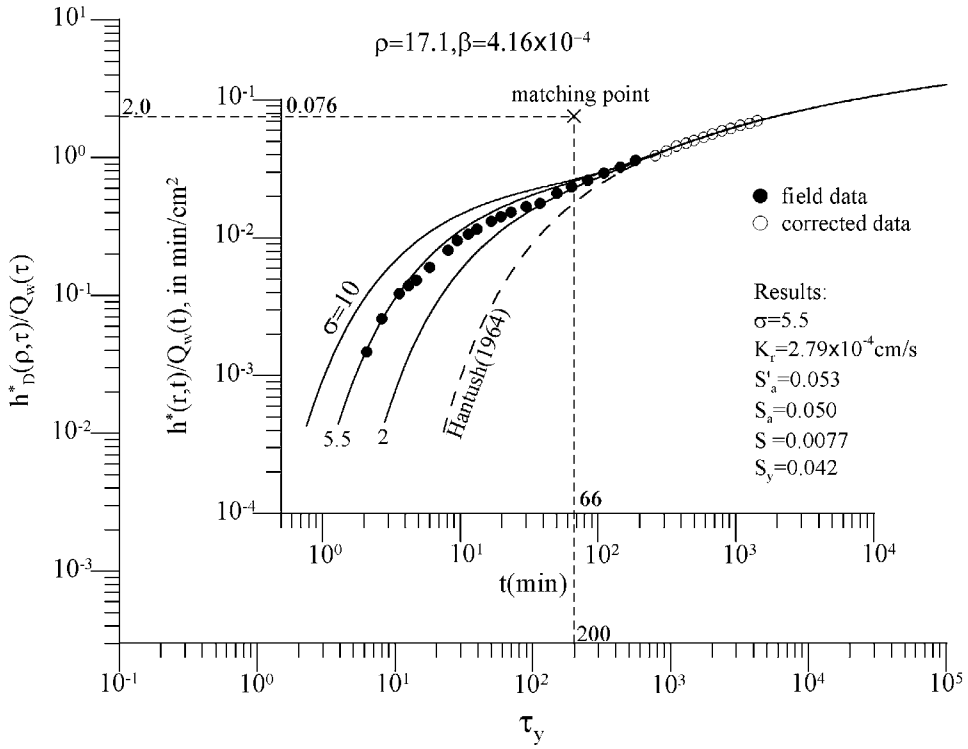

Figure 6. Using type A curves to match the field data to determine σ(=5.5) and the matching point.

[39] 2. Overlay the field data paper on top of the type curve paper, while keeping the abscissas and the ordinates parallel. Shift the field data curve to match one of the type A curves by fitting as many drawdown points of early times and late times as possible, ignoring the discrepancy in intermediate times. The type A curves shown in Figure 6 are obtained by trial and error by varying σ until the theoretical results compared reasonably

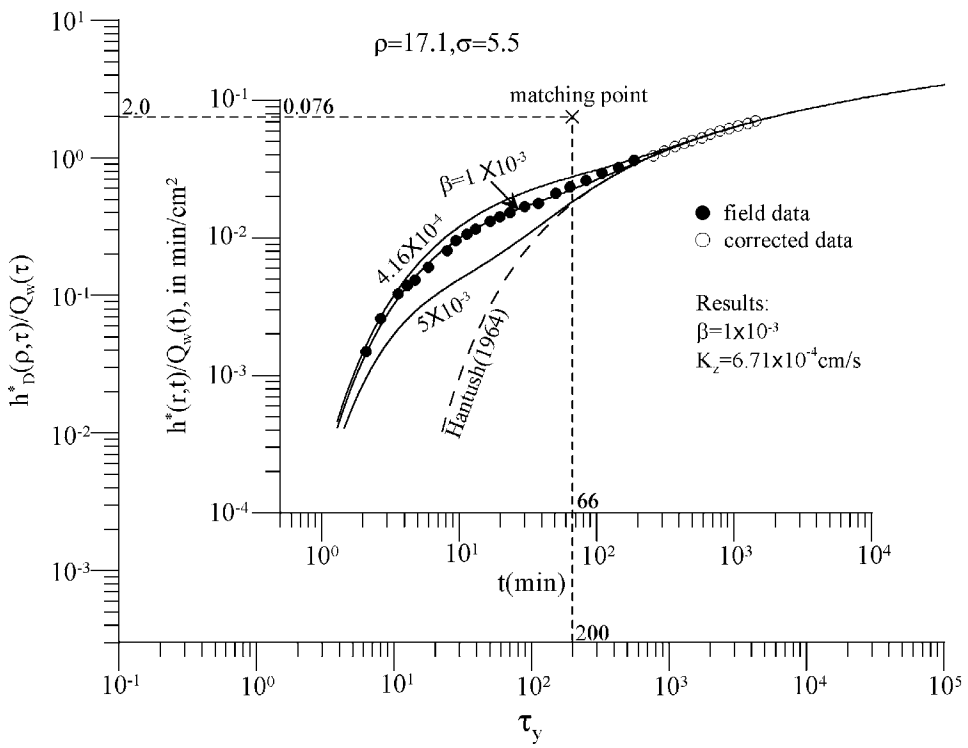

Figure 7. Using type B curves to match the field data to determine β(=1.0 × 10^{-3}) and the matching point.

Table 1. Data Analysis Results by the Curve Matching Method

r, cm	$K_r \times 10^{-4}$, cm/s	$K_z \times 10^{-4}$, cm/s	S_y	$S_s \times 10^{-5}$, cm^{-1}
87	2.79	6.71	0.042	3.08
180	3.21	4.63	0.020	1.88
271	3.37	3.40	0.014	1.76
362	4.16	3.50	0.015	2.64

well with most the early and late time data. The Hantush type curve is also exhibited to indicate the late time radial flow.

[40] 3. When matched, the σ value of the matched type curve is taken and a matching point on or off the matched curve is marked. The pair of (t, τ_y) and the pair of $[h^*(r, t)/Q_w(t), h_D^*(\rho, \tau)/Q_w(\tau)]$ associated with the matching point are located and read. Figure 6 shows that t = 66 min, $\tau_y = 200$, $h^*(r, t)/Q_w(t) = 0.076$ min/cm^2, and $h_D^*(\rho, \tau)/Q_w(\tau) = 2.0$.

[41] 4. Determine K_r using the pair of $[h^*(r, t)/Q_w(t), h_D^*(\rho, \tau)/Q_w(\tau)]$. That is, $h_D^*(\rho, \tau)/Q_w(\tau) = 2\pi K_r b h^*(r, t)/Q_w(t) = 2.0$, and hence K_r is 2.79×10^{-4} cm/s when $h^*(r, t)/Q_w(t) = 0.076$ min/cm^2. Accordingly, T is 0.07 cm^2/s as b is assumed to be 250 cm.

[42] 5. Determine S_a' from the pair of (t, τ_y) since the corrected drawdown data are used in late times (if no corrected drawdown is involved then the pair of (t, τ_y) yields S_a. That is, by letting $Tt/(r_w^2 S_a')$ to be 200, S_a' is 0.053 when t is 66 min. Since $S_a = 0.942 S_a'$, S_a is 0.05. Knowing that σ (i.e., S_y/S) is 5.5, one can find that S is 0.0077 and S_y is 0.042. Thus S_s is 3.08×10^{-5} cm^{-1}.

[43] 6. Prepare the type B curves for $\rho = 17.1$ and $\sigma = 5.5$, while allowing β to vary. By the same matching procedure as discussed above, the same field data curve is matched with one of the type B curves with an emphasis on the intermediate time section, as shown in Figure 7. The value of β is identified as 1.0×10^{-3}. With $(K_z r_w^2)/(K_r b^2)$ equal 1.0×10^{-3}, K_z is determined to be 6.71×10^{-4} cm/s.

3.2. Field Data Analysis and Discussion

[44] The curve matching method is applied to the four sets of drawdown data, and the results obtained are shown in Table 1. Accuracy of these estimates is validated in Figure 8, which demonstrates the good agreement between the field data and the theoretical responses calculated by using (8) and (9) with the parameter values listed in Table 1. Also shown is that the late time radial flow prevailed after about 260 minutes, as indicated by the Hantush type curve. The estimates of S_s are between 1.76×10^{-5} cm^{-1} and 3.08×10^{-5} cm^{-1}. They are smaller than the values ranging from 8.2×10^{-5} cm^{-1} to 1.6×10^{-4} cm^{-1} given

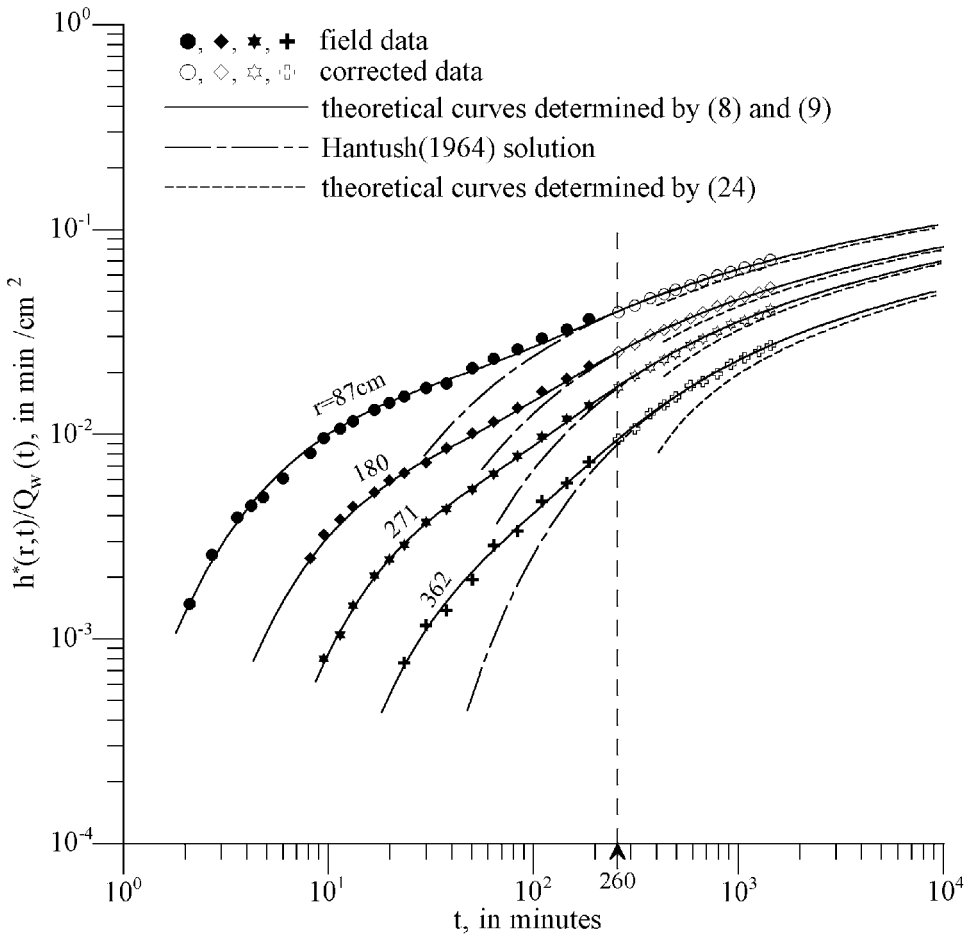

Figure 8. Validation of the accuracy of the estimates of the parameters and comparison of the field data with the type curves of *Hantush* [1964] solution and of the late time approximation of (24).

by *Grisak and Cherry* [1975], but are slightly larger than those ranging from 2.0×10^{-6} cm^{-1} to 1.1×10^{-5} cm^{-1} given by *Shaver* [1998]. The estimates of K_z and K_r are of the order of 10^{-4} cm/s. The range of K_r is from 2.79×10^{-4} cm/s to 4.16×10^{-4} cm/s, which are about two to three orders of magnitude higher than the values for unweathered till due to (1) a high sand content and a low clay content of the weathered till at the test site, and (2) the climatic factors that affect weathering of the till [*Jones*, 1993].

[45] The estimates of the four parameters show certain spatial variations (e.g., S_y decreases with the increasing distance, K_r increases with the increasing distance). This may be attributable to the field conditions that are not considered in the mathematical model; e.g., the drainage process associated with the water table decline is actually time dependent, saturated thickness varies significantly due to a relatively large h_w. Nevertheless, it is not uncommon that the estimates vary with distance, if the type curve analysis is applied to the individual set of drawdown data when more than one point of observation is available. *Moench* [1994] recommended a composite curve matching method, in which drawdown data from two or more observation wells are plotted against t/r^2 on one paper. This procedure considers the response of the aquifer as a whole and may obtain better "average" aquifer properties. The composite curve matching analysis for these observation wells is presented elsewhere.

[46] Figure 8 also shows that the 24 hour CHT was not long enough that any set of the late drawdown data had not been developed into the relation shown by (24). Therefore the well-known semilog method of determining T and S_a (or S_a') is not applicable to the late time data of the four wells.

4. Summary and Conclusion

[47] On the basis of this study, the following conclusions are drawn.

[48] 1. The three segments typically noted in the time drawdown history of a CRT are also characteristic of the time drawdown variation of a CHT. However, the early time and the late time segments conform to the solution given by *Hantush* [1964] for confined conditions in which the groundwater flow is purely radial. The early time radial flow segment is in terms of S, while the late time radial flow segment is in terms of an apparent storage coefficient as the sum of S and S_y.

[49] 2. During a CHT, both the constant head well discharge $Q_w(t)$ and aquifer drawdown $h^*(r, t)$ are continuously under the influence of well skin of the constant-head well, but $h^*(r, t)/Q_w(t)$ is free from the skin effect. It is suggested to use $h^*(r, t)/Q_w(t)$ for parameter estimation, especially when well skin is suspected to exist around the constant-head well.

[50] 3. A curve matching method using $h^*(r, t)/Q_w(t)$ is developed to determine S, S_y, K_r, and K_z. This method yields satisfactory results when it is applied to the field data of a 24-hour CHT performed in glacial till.

[51] 4. If h_w is not negligible in comparison to the initial saturated thickness, drawdown in late times may be large. Therefore it is required that the late drawdown data are corrected before the data analysis. It is shown that the Jacob correction is also applicable to the CHT.

Appendix A: Laplace Transform Solutions

[99] The dimensionless forms of (1) to (6) are:

$$\frac{\partial^2 h_D}{\partial \rho^2} + \frac{1}{\rho}\frac{\partial h_D}{\partial \rho} + \beta \frac{\partial^2 h_D}{\partial \zeta^2} = \frac{\partial h_D}{\partial \tau} \tag{A1}$$

$$h_D(\rho, \zeta, 0) = 0 \tag{A2}$$

$$\left[h_D - S_K \frac{\partial h_D}{\partial \rho}\right]_{\rho=1} = 1 \tag{A3}$$

$$h_D(\infty, \zeta, \tau) = 0 \tag{A4}$$

$$\left.\frac{\partial h_D}{\partial \zeta}\right|_{\zeta=0} = 0 \tag{A5}$$

$$\beta \left.\frac{\partial h_D}{\partial \zeta}\right|_{\zeta=1} = -\sigma \left.\frac{\partial h_D}{\partial \tau}\right|_{\zeta=1} \tag{A6}$$

[100] Application of the Laplace transform with respect to τ to (A1)–(A6) results in

$$\frac{\partial^2 H_D}{\partial \rho^2} + \frac{1}{\rho}\frac{\partial H_D}{\partial \zeta^2} + \beta \frac{\partial^2 H_D}{\partial \zeta^2} - pH_D = 0 \tag{A7}$$

$$\left[H_D - S_K \frac{\partial H_D}{\partial \rho}\right]_{\rho=1} = \frac{1}{p} \tag{A8}$$

$$H_D(\infty, \zeta, p) = 0 \tag{A9}$$

$$\left.\frac{\partial H_D}{\partial \zeta}\right|_{\zeta=0} = 0 \tag{A10}$$

$$\left.\frac{\partial H_D}{\partial \zeta}\right|_{\zeta=1} = -\frac{\sigma p}{\beta} H_D(\rho, 1, p) \tag{A11}$$

[101] Assuming that $H_D(\rho, \zeta, p)$ is the product of two distinct functions, $F(\rho, p)$ and $G(\zeta, p)$, one can transform (A7) to

$$\frac{1}{\beta F}\left[\frac{d^2 F}{d\rho^2} + \frac{1}{\rho}\frac{dF}{d\rho} - pF\right] = -\frac{1}{G}\frac{d^2 G}{d\zeta^2} \tag{A12}$$

and separates it into the following two equations

$$\frac{d^2 G}{d\zeta^2} + \varepsilon^2 G = 0 \tag{A13}$$

$$\frac{d^2 F}{d\rho^2} + \frac{1}{\rho}\frac{dF}{d\rho} - \chi^2 F = 0 \tag{A14}$$

where $\chi = (p + \beta\varepsilon^2)^{1/2}$, and ε is the separation constant. The solution of (A13) subject to (A10) is

$$G(\zeta, p) = a_1(p)\cos(|\varepsilon|\zeta) \tag{A15}$$

where $a_1(p)$ is constant. The solution of (A14) subject to (A9) is

$$F(\rho, p) = a_2(p)K_0(\chi\rho) \tag{A16}$$

where $a_2(p)$ is another constant. The product of (A15) and (A16) gives H_D as

$$H_D(\rho, \zeta, p) = A(p)K_0(\chi\rho)\cos(|\varepsilon|\zeta) \tag{A17}$$

where $A(p)$ is the constant product of $a_1(p)$ and $a_2(p)$. Substitution of (A17) into (A11) yields

$$\varepsilon(\tan\varepsilon) = \sigma p/\beta \tag{A18}$$

which has n's positive roots, ε_n, and n's negative roots, ε_n^-, n = 1, 2,.... Because $\varepsilon\tan(\varepsilon)$ is an even function, ε_n must be equal to - ε_n^-, or $|\varepsilon_n^-| = \varepsilon_n$.

[102] As a result, for any given root of (A18), there is a solution of $A_n(p)K_0(\chi_n\rho)\cos(\varepsilon_n\zeta)$ for (A17), n = 1, 2, 3..... The linear combination of all the n's solutions forms the complete solution for $H_D(\rho, \zeta, p)$,

$$H_D(\rho, \zeta, p) = \sum_{n=1}^{\infty} A_n(p)K_0(\chi_n\rho)\cos(\varepsilon_n\zeta) \tag{A19}$$

where $\chi_n = (p + \beta\varepsilon_n^2)^{1/2}$.

[103] The coefficients of $A_n(p)$ in (A19) are determined by substituting (A19) into (A8)

$$\sum_{n=1}^{\infty} A_n(p)[K_0(\chi_n) + S_k\chi_n K_1(\chi_n)]\cos(\varepsilon_n\zeta) = \frac{1}{p} \tag{A20}$$

Then, multiplying (A20) by $\cos(\varepsilon_m\zeta)$, where m is an integer, and integrating the multiplication results with respect to ζ over (0, 1), one obtains

$$\sum_{n=1}^{\infty} A_n(p)[K_0(\chi_n) + S_k\chi_n K_1(\chi_n)]\int_0^1 \cos(\varepsilon_n\zeta)\cos(\varepsilon_m\zeta)d\zeta = \frac{1}{p}\int_0^1 \cos(\varepsilon_m\zeta)d\zeta \tag{A21}$$

By (A18), the integral on the left-hand side of (A21) is evaluated as

$$\int_0^1 \cos(\varepsilon_n\zeta)\cos(\varepsilon_m\zeta)d\zeta = \begin{cases} \lambda_n \sin(2\varepsilon_n)/4\varepsilon_n & m = n \\ 0 & m \neq 0 \end{cases} \tag{A22}$$

where $\lambda_n = 1 + \sigma p/\beta + \varepsilon_n^2\beta/(\sigma p)$. Substitution of (A22) into (A21) gives

$$A_n(p) = \frac{2}{p}\frac{1}{K_0(\chi_n) + S_k\chi_n K_1(\chi_n)}\frac{1}{\lambda_n\cos\varepsilon_n} \tag{A23}$$

Finally, substitution of (A23) into (A19) gives (7).

Appendix B: Early Time and Late Time Approximations

B1. Early Time Drawdown Approximation

[104] When p is large as for τ being small, χ_n approaches $p^{1/2}$, and λ_n approaches $\sigma p/\beta$. By (A18), ε_n approaches $(n - 0.5)\pi$, and $\lambda_n\cos\varepsilon_n$ can be approximated by $\varepsilon_n\sin\varepsilon_n$, which is equal to $(-1)^{n-1}(n - 0.5)\pi$. Then, $H_D(\rho, \zeta, p)$ given by (7) reduces to

$$H_D(\rho, \zeta, p) = \frac{2}{p}\frac{K_0(\rho\sqrt{p})}{K_0(\sqrt{p}) + S_K\sqrt{p}K_1(\sqrt{p})} \cdot \sum_{n=1}^{\infty}(-1)^{n-1}\frac{\cos(n - 0.5)\pi\zeta}{(n - 0.5)\pi} \tag{B1}$$

The summation term can be calculated by using the following relation given by *Gradshteyn and Ryzhik* [1980, equation 0.232-2 and 1.442-4]

$$\sum_{n=1}^{\infty}(1)^{n-1}\frac{\cos(n - 0.5)\pi\zeta}{(n - 0.5)\pi} = \begin{cases} 0.5 & 0 \le \zeta < 1 \\ 0 & \zeta = 1 \end{cases} \tag{B2}$$

As a result, (B1) is simplified to (19) for $0 \le \zeta \le 1$, and to (20) for $\zeta = 1$.

B2. Late Time Drawdown Approximation

[105] When p is small as for large τ, ε_1 approaches $(\sigma p/\beta)^{1/2}$, χ_1 approaches $[p(1 + \sigma)]^{1/2}$, and λ_1 approaches 2. For $n > 1$, ε_n approaches $(n - 1)\pi$, χ_n approaches $\varepsilon_n\beta^{1/2}$, and λ_n approaches $\varepsilon_n^2\beta/\sigma p$. Then, $H(\rho, \zeta, p)$ given by (7) reduces to

$$H_D(\rho, \zeta, p) = \frac{1}{p}\left[\frac{K_0(\rho\sqrt{P})}{K_0(\sqrt{P}) + S_K\sqrt{P}K_1(\sqrt{P})} + 2p\sum_{n=2}^{\infty}\frac{\sigma(-1)^{n-1}K_0(\rho\chi_n)}{K_0(\chi_n) + S_K\chi_n K_1(\chi_n)}\frac{\cos\varepsilon_n\zeta}{\beta\varepsilon_n^2}\right] \tag{B3}$$

where $P = p(1 + \sigma)$. The vertical distance is only involved in the summation term, and thus this term deals with the influence of the vertical flow components. As p is small, the summation term is negligibly small relative to the first term, and the late time drawdown solution can be appropriately described by using the first term as shown in (21).

Notation

b	initial saturated thickness of aquifer, L.
h(r, z, t)	depth specific drawdown, L.
h*(r, t)	vertically averaged drawdown, L.
h_w	constant drawdown prescribed at the constant head well, L.
h′(r, t)	corrected late time drawdown, L.
H_w	corrected drawdown for h_w equal to h_w- (h_w^2/2b), L.
K_r	the horizontal hydraulic conductivity, L/T.
K_z	the vertical hydraulic conductivity, L/T.
$q_S(r, t)$	storage discharge, L/T.
$q_{Sy}(r, t)$	water table decline discharge, L/T.
$Q_w(t)$	constant-head well discharge, L^3/T.
$Q_S(t)$	total discharge from aquifer storage, L^3/T.
$Q_{Sy}(t)$	total discharge from the water table decline, L^3/T.

r	radial distance from the constant-head well, L
r_w	effective radius of the constant-head well, L.
S_s	specific storage, L^{-1}.
T	transmissivity equal to $K_r b$, L^2/T.
t	time since start of pumping, T.
z	vertical distance above bottom of aquifer, L.
$h_D(\rho, \zeta, \tau)$	$h(r, z, t)/h_w$, dimensionless.
$h_D^*(\rho, \tau)$	$h^*(r, t)/h_w$, dimensionless.
$H_D(\rho, \zeta, p)$	Laplace transform of $h_D(\rho, \zeta, \tau)$, dimensionless.
$h_e(\rho, \tau)$	dimensionless drawdown for small τ, dimensionless.
$h_l(\rho, \tau)$	dimensionless drawdown for large τ, dimensionless.
p	Laplace transform parameter of τ, dimensionless.
P	$p(1 + \sigma)$, dimensionless.
$q_S(\rho, \tau)$	$q_S(r, t)r_w^2/K_r b h_w$, dimensionless.
$q_{Sy}(\rho, \tau)$	$q_{Sy}(r, t)r_w^2/K_r b h_w$, dimensionless.
$Q_w(\tau)$	$Q_w(t)/2\pi K_r b h_w$, dimensionless.
$Q_S(\tau)$	$Q_S(t)/2\pi K_r b h_w$, dimensionless.
$Q_{Sy}(\tau)$	$Q_{Sy}(t)/2\pi K_r b h_w$, dimensionless.
S	storage coefficient, dimensionless.
S_a	apparent storage coefficient equal to $S + S_y$, dimensionless.
S_a'	$S_a b/(b - h)$, dimensionless.
S_y	specific yield, dimensionless.
S_k	skin factor, dimensionless.
β	$(K_z r_w^2)/(K_r b^2)$, dimensionless.
ρ	r/r_w, dimensionless.
σ	S_y/S, dimensionless.
τ	$(Tt)/(r_w^2 S)$, dimensionless.
τ_y	$(Tt)/(r_w^2 S_a)$, dimensionless.
ε_n	the nth positive root of (A18), dimensionless.
χ_n	$(p + \beta\varepsilon_n^2)^{1/2}$, dimensionless.
λ_n	$1 + p\sigma/\beta + \varepsilon_n^2\beta/(\sigma p)$, dimensionless.
ζ	z/b, dimensionless.

[106] **Acknowledgments.** The work presented is part of the project NSC-91-2116-M-008-007, supported by National Science Council. Special thanks are made to one anonymous reviewer and Allan Moench, who also provided us with the source code of his model, which helped us in writing our own. The Fortran program of the CHT solutions is available upon request.

References

Abdul, A. S., A new pumping strategy for petroleum product recovery from contaminated hydrogeologic systems: Laboratory and field evaluations, *Ground Water Monit. Rem.*, *12*, 105–114, 1992.

Akindunni, F. F., and R. W. Gillham, Unsaturated and saturated flow in response to pumping of an unconfined aquifer: Numerical investigation of delayed drainage, *Ground Water*, *30*(6), 873–884, 1992.

Bear, J., *Hydraulics of Groundwater*, 569 pp., McGraw-Hill, New York, 1979.

Boulton, N. S., Unsteady radial flow to a pumped well allowing for delayed yield from storage, in *General Assembly Rome*, tome II, *IASH Publ.*, *37*, 472–477, 1955.

Boulton, N. S., Analysis of data from non-equilibrium pumping tests allowing for delayed yield from storage, *Proc. Inst. Civ. Eng.*, *26*, 482–496, 1963.

Cassiani, G., Z. J. Kabala, and M. A. Medina Jr., Flowing partially penetrating well: Solution to a mixed-type boundary value problem, *Adv. Water Resour.*, *23*, 59–68, 1999.

Chang, C.-C., and C.-S. Chen, An integral transform approach for a mixed boundary problem involving a flowing partially penetrating well with infinitesimal well skin, *Water Resour. Res.*, *38*(6), 1071, doi:10.1029/2001WR001091, 2002.

Chang, C. C., and C. S. Chen, A flowing partially penetrating well in a finite-thickness aquifer: A mixed-type initial boundary value problem, *J. Hydrol.*, *271*, 101–118, 2003.

Chen, C.-S., and C.-C. Chang, Use of cumulative volume of constant-head injection test to estimate aquifer parameters with skin effects: Field experiment and data analysis, *Water Resour. Res.*, *38*(5), 1056, doi:10.1029/2001WR000300, 2002.

Chen, X. H., and J. F. Ayers, Aquifer properties determined from 2 analytical solutions, *Ground Water*, *36*(5), 783–791, 1998.

Churchill, R. V., *Operational Mathematics*, 481 pp., McGraw-Hill, New York, 1972.

Clegg, M. W., Some approximate solutions of radial flow problems associated with production at constant well pressure, *Soc. Pet. Eng. J.*, *240*, 31–42, 1967.

Cooper, H. H., and C. E. Jacob, A generalized graphical method for evaluating formation constants and summarizing well field history, *Eos Trans. AGU*, *27*, 526–534, 1946.

Dagan, G., A method of determining the permeability and effective porosity of unconfined anisotropic aquifers, *Water Resour. Res.*, *3*(4), 1059–1071, 1967.

Earlougher, R. C. Jr., *Advances in Well Test Analysis*, *Monogr. Ser.*, vol. 5, Soc. of Pet. Eng., Dallas, Tex., 1977.

Gambolati, G., Transient free surface flow to a well: An analysis of theoretical solutions, *Water Resour. Res.*, *12*(1), 27–39, 1976.

Gradshteyn, I. S., and I. M. Ryzhik, *Table of Integrals, Series, and Products*, 1160 pp., Academic, San Diego, Calif., 1980.

Grisak, G. E., and J. A. Cherry, Hydrologic characteristics and response of fractured till and clay confining a shallow aquifer, *Can. Geotech. J.*, *12*(24), 23–42, 1975.

Hantush, M. S., Hydraulics of wells, in *Advances in Hydroscience*, vol. 1, edited by V. T. Chow, pp. 281–432, Academic, San Diego, Calif., 1964.

Hiller, C. K., and B. S. Levy, Estimation of aquifer diffusivity from analysis of constant-head pumping test data, *Ground Water*, *32*(1), 47–52, 1994.

Hurst, W., J. D. Clark, and E. B. Brauer, The skin effect in producing wells, *J. Pet. Technol.*, *246*, 1483–1489, 1969.

Jacob, C. E., Notes on determining permeability by pumping tests under watertable conditions, open file report, 34 pp., U. S. Geol. Surv., Reston, Va., 1944.

Jacob, C. E., and S. W. Lohman, Nonsteady flow to a well of constant drawdown in an extensive aquifer, *Eos Trans. AGU*, *33*(4), 559–569, 1952.

Jargon, J. R., Effect of wellbore storage and wellbore damage at the active well on interference test analysis, *J. Pet. Technol.*, *28*, 851–858, 1976.

Jones, L., A comparison of pumping and slug tests for estimating the hydraulic conductivity of unweathered Wisconsin age till in Iowa, *Ground Water*, *31*(6), 896–904, 1993.

Jones, L., T. Lemar, and C.-T. Tsai, Results of two pumping tests in Wisconsin age weathered till in Iowa, *Ground Water*, *30*(4), 529–538, 1992.

Mishra, S., and D. Guyonnet, Analysis of observation-well response during constant-head testing, *Ground Water*, *30*(4), 523–528, 1992.

Moench, A. F., Specific yield as determined by type-curve analysis of aquifer-test data, *Ground Water*, *32*(6), 949–957, 1994.

Moench, A. F., Combining the Neuman and Boulton models for flow to a well in an unconfined aquifer, *Ground Water*, *33*(3), 378–384, 1995.

Moench, A. F., Flow to a well of finite diameter in a homogeneous, anisotropic water table aquifer, *Water Resour. Res.*, *33*(6), 1397–1407, 1997.

Moench, A. F., S. P. Garabedian, and D. R. LeBlanc, Estimation of hydraulics parameters from an unconfined aquifer test conducted in a glacial outwash deposit, Cape Cod, Massachusetts, *U.S. Geol. Surv. Prof. Pap.*, *1629*, 69 pp., 2001.

Mucha, I., and E. Paulikova, Pumping test using large-diameter production and observation wells, *J. Hydrol.*, *89*, 157–164, 1986.

Murdoch, L. C., and J. Franco, The analysis of constant drawdown wells using instantaneous source functions, *Water Resour. Res.*, *30*(1), 117–124, 1994.

Narasimhan, T. N., and M. Zhu, Transient flow of water to a well in an unconfined aquifer: Applicability of some conceptual models, *Water Resour. Res.*, *29*(1), 179–191, 1993.

Neuman, S. P., Theory of flow in unconfined aquifers considering delayed response of the water table, *Water Resour. Res.*, *8*(4), 1031–1044, 1972.

Neuman, S. P., Effects of partial penetration on flow in unconfined aquifers considering delayed aquifer response, *Water Resour. Res.*, *10*(2), 303–312, 1974.

Neuman, S. P., Analysis of pumping test data from anisotropic unconfined aquifers considering delayed gravity response, *Water Resour. Res.*, *11*(2), 329–342, 1975.

Nwankwor, G. I., R. W. Gillham, G. van der Kamp, and F. F. Akindunni, Unsaturated and saturated flow in response to pumping of an unconfined aquifer: Field evidence of delayed drainage, *Ground Water*, *30*(5), 690–700, 1992.

Schapery, R. A., Approximate methods of transform inversion for viscoelastic stress analysis, in *Proceedings of 4th U. S. National Congress of Applied Mechanics*, pp. 1075–1085, Univ. Calif. Press, Berkeley, 1961.

Shaver, R. B., The determination of glacial till specific storage in North Dakota, *Ground Water*, *36*(4), 552–557, 1998.

Stehfest, H., Numerical inversion of Laplace transforms, *Commun. ACM*, *13*, 47–49, 1970.

Uraiet, A. A., and R. Raghavan, Unsteady flow to a well producing at a constant pressure, *J. Pet. Technol.*, *32*(10), 1803–1812, 1980.

C.-C. Chang and C.-S. Chen, Institute of Applied Geology, National Central University, 300, Jung-da Road, Chung-li, Taiwan 320. (chenchia@cc.ncu.edu.tw)